Ability of a "minimum" microbial food web model to reproduce response patterns observed in mesocosms manipulated with N and P, glucose, and Si

T. Frede Thingstad [a,*], Harry Havskum [b], Ulla Li Zweifel [c], Elisa Berdalet [d], M. Montserrat Sala [d], Francesc Peters [d], Miquel Alcaraz [d], Renate Scharek [d], Maite Perez [e], Stéphan Jacquet [f,1], Gro Anita Fonnes Flaten [a], John R. Dolan [e], Celia Marrasé [d], Fereidoun Rassoulzadegan [e], Åke Hagstrøm [c], Daniel Vaulot [f]

[a] Department of Biology, University of Bergen, Jahnebakken 5, N-5020 Bergen, Norway
[b] Marine Biological Laboratory, University of Copenhagen, Strandpromenaden 5, DK-3000 Helsingør, Denmark
[c] Kalmar University, Department of Natural Sciences, Smålandsgatan 24, Norra Vägen P.O. Box 905, S-39129 Kalmar, Sweden
[d] Institut de Ciències del Mar, CMIMA (CSIC), Passeig Marítim de la Barceloneta 37-49, E-08003 Barcelona, Catalunya, Spain
[e] Université Paris6, Laboratoire d'Océanographie de Villefranche UMR CNRS 7093, Marine Microbial Ecology Group, Station Zoologique, BP 28, F-06230 Villefranche-sur-Mer, France
[f] Station Biologique, Université Pierre et Marie Curie (Paris VI), BP 74, F-29682 Roscoff Cx, France

Abstract

We compared an idealised mathematical model of the lower part of the pelagic food web to experimental data from a mesocosm experiment in which the supplies of mineral nutrients (nitrogen and phosphorous), bioavailable dissolved organic carbon (BDOC, as glucose), and silicate were manipulated. The central hypothesis of the experiment was that bacterial consumption of BDOC depends on whether the growth rate of heterotrophic bacteria is limited by organic-C or by mineral nutrients. In previous work, this hypothesis was examined qualitatively using a conceptual food web model. Here we explore the extent to which a "simplest possible" mathematical version of this conceptual model can reproduce the observed dynamics. The model combines algal–bacterial competition for mineral nutrients (phosphorous) and accounts for alternative limitation of bacterial and diatom growth rates by organic carbon and by silicate, respectively. Due to a slower succession in the diatom–copepod, compared to the flagellate–ciliate link, silicate availability increases the magnitude and extends the duration of phytoplankton blooms induced by mineral nutrient addition. As a result, Si interferes negatively with bacterial consumption of BDOC consumption by increasing and prolonging algal–bacterial competition for mineral nutrients. In order to reproduce the difference in primary production between Si and non-Si amended treatments, we had to assume a carbon overflow mechanism in diatom C-fixation. This model satisfactorily reproduced central features observed in the mesocosm experiment, including the dynamics of glucose consumption, algal, bacterial, and mesozooplankton biomass. While the parameter set chosen allows the model to reproduce the pattern seen in bacterial production, we were not able to find a single set of parameters that simultaneously reproduces both the level and the pattern observed for bacterial production. Profound changes in bacterial morphology and stoichiometry were reported in glucose-amended

---

* Corresponding author.
  E-mail address: frede.thingstad@bio.uib.no (T.F. Thingstad).
[1] Present address: Station INRA d'Hydrobiologie Lacustre, UMR CARRTEL, BP 511, 74203 Thonon, France.

mesocosms. Our "simplest possible" model with one bacterial population with fixed stoichiometry cannot reproduce this, and we suggest that a more elaborate representation of the bacterial community is required for more accurate reproduction of bacterial production.

1. Introduction

Relatively simple models with a linear nutrient–phytoplankton–zooplankton food chain reflect many essential aspects of the pelagic ecosystem. Such linear food chain models, however, do not exploit the insight gained over the last two decades concerning the activities and importance of marine microbes. Attempts have been made to account for small organisms by arranging groups of phytoplankton and zooplankton according to size (Moloney and Field, 1991) but these neglect heterotrophic bacteria. These organisms have long been recognised as playing a central role in the pelagic carbon cycle (Pomeroy, 1974; Williams, 1981; Azam et al., 1983) and need also to be included in such structures, in particular if the aim is an understanding of the pelagic C-cycle. Over 20 years ago, in the description of the microbial loop (Azam et al., 1983), bacterial carbon demand was recognised as potentially controlled by interactions between distinct factors such as bacterial physiology, predation, nutrient competition, and autochthonous release of dissolved organic matter from the food web.

The importance of heterotrophic bacteria in marine food webs is today generally accepted and it is recognised that a substantial fraction of the flow of inorganic nutrients may enter the particulate food web via heterotrophic bacteria (Rigler, 1956; Harrison et al., 1977; Wheeler and Kirchman, 1986; Suttle et al., 1990; Kirchman, 1994). More recently, experimental evidence has also accumulated for a widespread occurrence of situations where bacterial growth may be limited by mineral nutrients (e.g. N or P) rather than by organic carbon (Pomeroy et al., 1995; Rivkin and Anderson, 1997; Zohary and Robarts, 1998; Sala et al., 2002; Van Wambeke et al., 2002).

As one tool in the search for a deeper understanding of the nature of the microbial part of the pelagic food web, many authors have used mathematical models that focus on various aspects of bacterial growth and transformation of matter (Billen and Servais, 1989; Fasham et al., 1990; Taylor and Joint, 1990; Baretta-Bekker et al., 1995; Vallino et al., 1996; Baretta-Bekker et al., 1997; Thingstad et al., 1999a,b; Van den Meersche et al., 2004). Since we now know that bacterial growth in natural communities can be limited alternatively by mineral nutrients or by organic carbon (Thingstad and Lignell, 1997), a
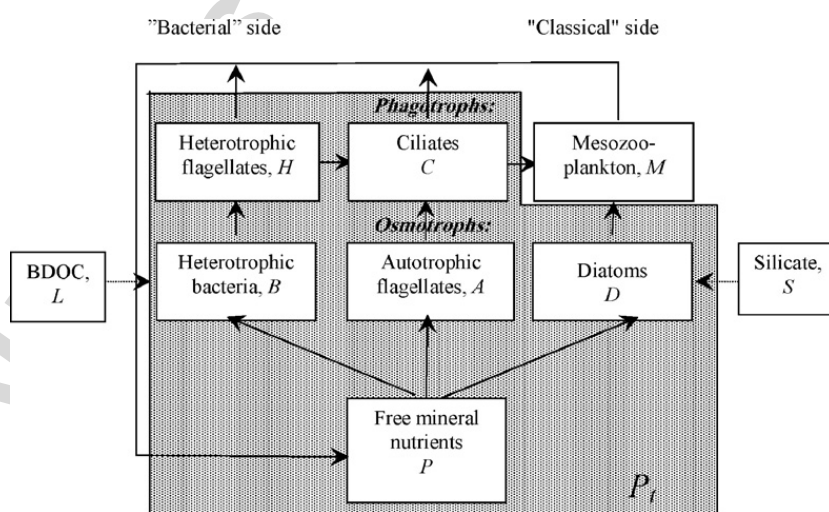

Fig. 1. Flow structure for mineral nutrient (phosphorous used in model description) through the "minimum" model food web. Three functional groups of osmotrophic organisms compete for the common mineral nutrient, three functional groups of phagotrophs prey selectively on these competitors. The partitioning of flows is potentially influenced by BDOC and silicate, allowing for the possibilities of C-limitation and Si-limitation of bacterial and diatom growth rates, respectively. The shaded area, containing a total phosphorous concentration P_t, corresponds to what is termed "the microbial part of the system" in the text. This part is assumed to be in internal steady state at time=0.

fundamental requirement for any model aspiring to give a generic description of bacterial growth is thus the capability to cope satisfactorily with *both* of these situations.

Idealised models that contain sufficient elements to allow for shifts between carbon and mineral nutrient limited bacterial growth have been proposed in several contexts (Thingstad and Pengerud, 1985; Thingstad et al., 1997), also including a potential alteration of the level of algal–bacterial nutrient competition by Si-requiring diatoms (Thingstad and Rassoulzadegan, 1999; Havskum et al., 2003; Thingstad, 2003). The underlying principle of these models is that mineral nutrient limited bacteria are "sandwiched" between protozoan predators that control their biomass (B), and phytoplankton competitors that control their growth rate (μ_B) via the common limiting mineral nutrient, the result being a combined control restricting bacterial production ($\mu_B B$) (Thingstad and Lignell, 1997).

Although models have been used to analyze experimental situations with shifts in limitation (Thingstad et al., 1999b), we are not aware of any critical attempt to evaluate the properties required of a model aspiring to cover both situations. Here we compare just such a model to experimental data from a mesocosm experiment in which the supplies of mineral nutrients (nitrogen and phosphorous), bioavailable dissolved organic carbon (BDOC, as glucose), and silicate were manipulated.

The mesocosm experiment has been previously described (Jacquet et al., 2002; Havskum et al., 2003). It was started from an initial state with C-limited bacterial growth rate. With nutrient manipulations involving glucose (potentially relieving bacterial C-limitation), mineral N and P (potentially inducing a transient autotroph–heterotroph succession), and Si (potentially increasing algal–bacterial competition for mineral nutrient due to the build-up of a high osmotroph biomass in diatoms), the experiment covered different combinations of factors limiting microbial growth rate, different succession patterns, and different size structures of the microbial food web. It thus provided an unusually diverse set of situations with which a model can be challenged.

The aim of the work reported here is to explore the extent to which a "simplest possible" mathematical version of the idealised conceptual version of the model as used in a qualitative manner by Havskum et al. (2003), can reproduce the level and the temporal dynamics observed in this mesocosm experiment.

2. Model and model philosophy

At the present state of the art we regard an identification of the set of main controlling mechanisms to be

Table 1
Equations describing the steady state of the microbial subsystem

Assuming food intake to be proportional to food concentration, the steady state requirement of Growth = Loss for all microbial variables gives:

For bacterial biomass B:

$$\alpha_{BP}P^*B^* = \alpha_H B^* H^* \quad \text{if } \alpha_{BP}P^* \leq \alpha_{BL}L^* \text{ (P–limitation)} \tag{1A}$$

$$Y_{BC}\Psi = \alpha_H B^* H^* = \alpha_{BC}L^* B^* \quad \text{if } \alpha_{BP}P^* > \alpha_{BL}L^* \text{ (C–limitation).} \tag{1B}$$

For autotrophic flagellates:

$$\alpha_{AP}P^*A^* = \alpha_C A^* C^*. \tag{2}$$

For diatoms:

$$\alpha_{DP}P^*D^* = \alpha_M D^* M \quad \text{if } \alpha_{DP}P^* \leq \alpha_{DS}S^* \tag{3A}$$

$$\alpha_{DS}Si^*D^* = \alpha_M D^* M \quad \text{if } \alpha_{DP}P^* > \alpha_{DS}S^*. \tag{3B}$$

For heterotrophic flagellates:

$$Y_H \alpha_H B^* H^* = \alpha_C H^* C^*. \tag{4}$$

For ciliates:

$$Y_C \alpha_C (H^* + A^*)C^* = \alpha_M CM^*. \tag{5}$$

Mass balances for nitrogen and silicate give:

$$P^* + B^* + A^* + D^* + H^* + C^* = P_t. \tag{6}$$

$$D^* \rho_{DS}^{-1} + S^* = S_T. \tag{7}$$

See Table 4 for symbol description.

more important than adding numerous elements to obtain a perfect numerical fit between observations and model. The food web structure used is redrawn in Fig. 1 from Havskum et al. (2003). With three predator populations (heterotrophic flagellates, ciliates and mesozooplankton), this structure has enough elements to include the selective predation required to maintain coexistence between three groups of osmotroph competitors (heterotrophic bacteria, autotrophic flagellates, and diatoms). When there is more labile dissolved organic carbon (BDOC) and more free silicate in the water than the organisms can consume, all osmotrophs will be mineral nutrient limited and there will be one flow pattern for the limiting element (represented as phosphorous) through the food web. This flow pattern depends upon a balance determined by the relative magnitude of organism properties such as uptake affinities and clearance rates (see steady state analysis below). When

Table 2
Some properties of the steady state when all osmotrophs are P-limited

As long as ciliates are present ($C^* > 0$), the sum of flagellates ($H^* + A^*$) is always proportional to ciliate loss rate $\sigma \alpha_M M$ (from Eq. (5)):

$$H^* + A^* = \frac{\sigma \alpha_M}{Y_C \alpha_C} M. \tag{8}$$

As long as heterotrophic flagellates are present ($H^* > 0$), bacterial biomass is always proportional to the biomass of ciliates (from Eq. (4)),

$$B^* = \frac{\alpha_C C^*}{Y_H \alpha_H}. \tag{9}$$

As long as autotrophic flagellates are present, ciliates (C^*) and free mineral nutrients (P^*) are proportional (from Eq. (2)).

$$C^* = \frac{\alpha_{AP}}{\alpha_C} P^* \tag{10}$$

A similar argument relates heterotrophic flagellates (H^*) to free mineral nutrients (P^*) (from Eq. (1A)):

$$H^* = \frac{\alpha_{BP}}{\alpha_H} P^* \tag{11}$$

When diatoms are present ($D^* > 0$) and P-limited, Eq. (3A) is valid, and:

$$P^* = \frac{\alpha_M}{\alpha_{DP}} M. \tag{12}$$

Eqs. (11) and (12) can be inserted into Eq. (8) to give A^*:

$$A^* = \left[\frac{\sigma}{Y_C \alpha_C} - \frac{\alpha_{BP}}{\alpha_H \alpha_{DP}} \right] \alpha_M M. \tag{13}$$

In the case of diatoms present and all osmotrophs N-limited, all state variables P^*, B^*, A^*, H^*, and C^*, become proportional to mesozooplankton biomass M. Insertion of this into the mass balance requirement Eq. (6), steady state diatom biomass becomes a linear function of total nutrient content P_t and M:

$$D^* = P_t - \left[\frac{\sigma}{\alpha_C} - \left(1 + \left(1 + \frac{\alpha_C}{Y_H \alpha_H} \right) \frac{\alpha_{AP}}{\alpha_C} \right) \frac{1}{\alpha_{DP}} \right] \alpha_M M. \tag{14}$$

Since both B^* and P^* are proportional to M when both diatoms (Eq. (3A) valid) and bacteria (Eq. (1A) valid) are P-limited, bacterial production (BP_P) become proportional to the 2nd power of M:

$$BP_P^* = \alpha_{BP} P^* B^* = Y_H^{-1} \frac{\alpha_{BP} \alpha_{AP}}{\alpha_H \alpha_{DP}^2} \alpha_M^2 M^2. \tag{15}$$

Using Eq. (14), we see that the possibility for diatoms to establish in the system ($D^* > 0$) depends on the partitioning of the limiting element between the microbial part of the system (P_t) and mesozooplankton (M). The critical value for this ratio, below which diatoms disappear from the system is (obtained by setting $D^* = 0$ in Eq. (14)) :

$$(P_t/M)^{\text{crit}} = \left(\frac{\sigma}{\alpha_C} - \left(1 + \left(1 + \frac{\alpha_C}{Y_H \alpha_H} \right) \frac{\alpha_{AP}}{\alpha_C} \right) \frac{1}{\alpha_{DP}} \right) \alpha_M \tag{16}$$

heterotrophic bacteria become C-limited or diatoms Si-limited, flow into the food web's left "bacterial" or its right "classical" side, respectively, will be restricted. This proposed idealisation of the food web thus bestows a somewhat symmetric role to BDOC and silicate in their control of the food web flow pattern.

Mathematical descriptions basically using Lotka–Volterra type formulations to represent microbial food webs have been demonstrated to be powerful enough to explain some of the essential features of nutrient-manipulated mesocosms (Thingstad et al., 1999a,b) characterised by phosphorous-limited growth rate of both phytoplankton and heterotrophic bacteria. Starting with a combination of C-limited bacteria and the presence of free silicate (Jacquet et al., 2002; Havskum et al., 2003), the initial state of the mesocosm experiment used here for model comparison differed considerably from those previously analysed where bacteria were initially P-limited and the models used did not contain diatoms (Thingstad et al., 1999a,b).

A simulation model can be tuned to fit experimental data in three ways: 1) by modifying the structure of the model, 2) by modifying the numerical values of model parameters, and 3) by modifying the initial values of the state variables. With so many degrees of freedom, anyone that has attempted to model natural ecosystems will probably have experienced the feeling of building castles on a sandy foundation. The degrees of freedom can be reduced considerably if, at the start of the experiment, the microbial part of the food web (shaded area in Fig. 1) can be considered to be in internal steady state. In our

Table 3
Steady state when bacteria are C-limited

Carbon-limited bacterial production BP_C is given by (from Eq. (1B)):

$$BP_C^* = Y_{BC} \Psi. \tag{17}$$

Bacterial production realised at steady state must be the smallest of the two values BP_C^* and BP_P^*. This can be summarised in a dimensionless limitation index $\eta = BP_P^* / BP_C^*$. Bacteria will be carbon-limited if $\eta > 1$, P-limited if $\eta < 1$. Combining Eqs. (15) and (17) gives:

$$\eta = Y_{BC}^{-1} Y_H^{-1} \frac{\alpha_{BP} \alpha_{AP}}{\alpha_H \alpha_{DP}^2} \frac{\alpha_M^2}{\Psi} M^2 \quad \text{for } D^* > 0 \text{ and } S^* > \frac{\alpha_{DP}}{\alpha_{DS}} P^*. \tag{18}$$

The same type of arguments can be used to derive a somewhat more complex expression for η in cases with diatoms present but Si-limited, or when diatoms are absent (not shown).

Carbon limited bacterial growth rate combined with diatoms present and P-limited imply that (from Eq. (1B))

$$H^* = \frac{Y_{BC} \Psi}{\alpha_H B^*} = Y_{BC} Y_H \frac{\alpha_{DP}}{\alpha_{AP}} \frac{\Psi}{\alpha_M M} \tag{19}$$

H^* in this case thus increases in proportion to organic supply Ψ and decreases with mesozooplankton predation pressure. Increases/decreases in H^* will have corresponding decreases/increases in A^* as determined by Eq. (13).

When bacterial growth rate is C-limited, there is also a steady state condition for the BDOC pool:

$$L^* = \frac{Y_{BC} \Psi}{\alpha_{BC} B} \tag{20}$$

Table 4
List of symbols

Symbol	Meaning	Initial/parameter value	Unit
State variables (superscript "" used to denote steady state values)*			
B	Biomass bacteria	From Eq. (9)	nmol-P L^{-1}
A	Biomass autotrophic flagellates	From Eq. (13)	nmol-P L^{-1}
D	Biomass diatoms	From Eq. (14)	nmol-P L^{-1}
H	Biomass heterotrophic flagellates	From Eq. (8)	nmol-P L^{-1}
C	Biomass ciliates	From Eq. (10)	nmol-P L^{-1}
M	Biomass mesozooplankton	40	nmol-P L^{-1}
P	Free bioavailable phosphate	From Eq. (12)	nmol-P L^{-1}
L	Bioavailable dissolved organic carbon (BDOC)	From Eq. (20)	nmol-C L^{-1}
S	Free silicate	4000	nmol-Si L^{-1}
Affinities, clearance rates			
α_{BP}	Bacterial affinity for P	0.08	L nmol-P^{-1} h^{-1}
α_{BL}	Bacterial affinity for L	5.3 10^{-6}	L nmol-P^{-1} h^{-1}
α_{AP}	Autotrophic flagellate affinity of for P	0.04	L nmol-P^{-1} h^{-1}
α_{DP}	Diatom affinity for P	0.03	L nmol-P^{-1} h^{-1}
α_{DS}	Diatom affinity for S	0.0012	L nmol-P^{-1} h^{-1}
α_H	Heterotrophic flagellate clearance rate for bacteria	0.0015	L nmol-P^{-1} h^{-1}
α_C	Ciliate clearance rate for auto- and heterotrophic flagellates	0.0005	L nmol-P^{-1} h^{-1}
α_M	Mesozooplankton clearance rate for diatoms	0.00015	L nmol-P^{-1} h^{-1}
σ	Mesozooplankton selectivity factor for ciliates relative to diatoms	2	Dimensionless
Maximum growth rates			
μ_B^m	Maximum growth rate B	0.25	h^{-1}
μ_A^m	Maximum growth rate A	0.054	h^{-1}
μ_D^m	Maximum growth rate D	0.063	h^{-1}
μ_H^m	Maximum growth rate H	0.1	h^{-1}
μ_C^m	Maximum growth rate C	0.05	h^{-1}
μ_M^m	Maximum growth rate M	0.00625	h^{-1}
Yields			
Y_{BC}	Bacterial yield on L	0.004	nmol-P nmol-C^{-1}
Y_H	Heterotrophic flagellate yield on bacteria	0.3	nmol-P nmol-P^{-1}
Y_C	Ciliate yield on auto- and heterotrophic flagellates	0.2	nmol-P nmol-P^{-1}
Y_M	Mesozooplankton yield on ciliates and diatoms	0.15	nmol-P nmol-P^{-1}
Forcing parameters for microbial part of the system			
Ψ	Supply rate of L		nmol-C L^{-1}h^{-1}
P_t	Total -P in microbial part of the food web	220	nmol-P L^{-1}
S_t	Total bioavailable silicium		nmol-Si L^{-1}
Stoichiometric ratios and conversion factors:			
ρ_B	Molar carbon:phosphorous ratio in bacteria	50	nmol-C nmol-P^{-1}
ρ_A	Molar carbon:phosphorous ratio in phytoplankton	106	nmol-C nmol-P^{-1}
ρ_{DS}	Molar phosphorous:silicate ratio of diatoms	0.04	nmol-Si nmol-P^{-1}
ρ_{Chl}	Carbon:chlorophyll ratio (w:w)	60	
Others			
γ	Fraction of consumed diatom Si that is remineralised to free Si	0.25	Dimensionless
ε_A	Autotrophic flagellate ability to turn off excess C-fixation	1	Dimensionless
ε_D	Diatom ability to turn off excess C-fixation	0	Dimensionless
k	Proportionality constant between production of L and P_T^2	1.1 10^{-4}	nmol-C L^{-1} h^{-1} (nmol-P L^{-1})$^{-2}$
δ_M	Loss rate of mesozooplankton	0	d^{-1}
η	Limitation index (from Eq. (18))	9.6	Dimensionless
E_{Li}	Experimental input rate of L, $i=1...10$ for the 10 different mesocosm treatments	See Table 5	nmol-C L^{-1}h^{-1}
E_{Si}	Experimental input rate of S, $i=1...10$ for the 10 different mesocosm treatments	See Table 5	nmol-Si L^{-1}h^{-1}
E_{Pi}	Experimental input rate of P, $i=1...10$ for the 10 different mesocosm treatments	See Table 5	nmol-P L^{-1}h^{-1}

Table 5

Codes used for the 10 different mesocosm manipulations simulated

Eight mesocosms forming two gradients, parallel in daily glucose additions

C-gradient No Si added	CSi-gradient Si kept replete by additions starting after 3.5 d	Glucose-C added μmol m^{-3} d^{-1}
C_0	C_0Si	0
C_1	C_1Si	10600
C_3	C_3Si	31800
C_{10}	$C_{10}Si$	106000

Two control mesocosms receiving no mineral nutrients

K	0
KC_{10}	106000

Eight of these received a daily dose of 100 μmol PO$_4$–P and 1600 μmol NO$_3$–N m^{-3} d^{-1} and was split into two series (C_0–C_{10}, and CSi_0–CSi_{10}) forming gradients identical in their glucose addition, but differing in their Si-addition after day 3.5 by Si being depleted by diatom growth in the C-series, while Si was kept replete in the CSi-series. The two remaining treatments were one control without any additions (K) and one with only the 10× Redfield addition of glucose (KC_{10}).

mesocosm experiment, temporal changes in the control mesocosms were small, indicating that such an assumption is a valid first approximation. In addition to the requirement that the model should be able to reproduce the response patterns observed to different manipulations, we then also have the condition that it should be able to produce an initial steady state in reasonable agreement with observations.

2.1. The initial steady state

If we make the assumption that all populations in the microbial part of the system are food limited at steady state, so that food uptake can be considered proportional to food concentration, the analytical solution to a Lotka–Volterra representation of the system (Table 1) is fairly easy to derive (Tables 2 and 3). This solution expresses all state variables in terms of the two forcing variables: 1) total phosphate in the microbial part of the system (P_t) and 2) phosphate in mesozooplankton (M). The solution contains a set of "physiological parameters" characterising the organisms (symbols and parameter values summarised in Table 4). These are the proportionality constants between food concentration and food consumption (α-parameters), and the yield parameters (Y-parameters), that represent the fraction of limiting element in prey that is incorporated into the predator. Also, Y_{BC}, and ρ_{DS} represent the stoichiometric coupling between consumption of BDOC and silicate, and the formation of bacterial and diatom biomass, respectively.

The steady state is computed with the supply rate (Ψ) of BDOC as an independent parameter. Note that the steady state requirements for bacteria (Eqs. (1A) and (1B)) and for diatoms (Eqs. (3A) and (3B)) each lead to two alternative equations, depending upon the type of growth rate limitations (mineral nutrient (P) or BDOC (L) for bacteria, mineral nutrient (P) or silicate (S) for diatoms).

Table 2 gives the steady-state solution for the case when all organism groups are present, and all osmotrophs (bacteria, autotrophic flagellates, and diatoms) are P-limited. Diatom presence and dominance in the initial community then depends on the ratio (P_t:M) between the two forcing variables (Table 2 Eqs. (14) and (16)). Relative dominance between diatoms and autotrophic flagellates in the initial community is thus an emergent property of the initial value

Table 6

Differential equations used for simulating the response to nutrient manipulations in each mesocosm

$$\frac{dB}{dt} = \mu_B B - Y_H^{-1} \mu_H H \tag{21}$$

$$\frac{dA}{dt} = \mu_A A - \frac{A}{A+H} Y_C^{-1} \mu_C C \tag{22}$$

$$\frac{dD}{dt} = \mu_D D - \frac{D}{D+\sigma C} Y_M^{-1} \mu_M M \tag{23}$$

$$\frac{dH}{dt} = \mu_H H - \frac{H}{A+H} Y_C^{-1} \mu_C C \tag{24}$$

$$\frac{dC}{dt} = \mu_C C - \frac{\sigma C}{D+\sigma C} Y_M^{-1} \mu_M M \tag{25}$$

$$\frac{dM}{dt} = \mu_M M - \delta_M M \tag{26}$$

$$\frac{dP}{dt} = \frac{(1-Y_H)}{Y_H} \mu_H H + \frac{1-Y_C}{Y_C} \mu_C C + \frac{1-Y_M}{Y_M} \mu_M M$$
$$- \mu_B B - \mu_A A - \mu_D D + E_{Pi}$$

$$\frac{dL}{dt} = k(P_t + M)^2 - Y_{BC}^{-1} \mu_B B + E_{Li} \tag{28}$$

$$\frac{dS}{dt} = \rho_{DS}^{-1} \left(Y_M^{-1} \frac{D}{D+\sigma C} \mu_M M - \mu_D DM \right) + E_{Si} \tag{29}$$

$$\mu_B = \min(\alpha_{BP} P, \alpha_{BL} L, \mu_B^m) \tag{30}$$

$$\mu_A = \min(\alpha_{AP} P, \mu_A^m) \tag{31}$$

$$\mu_D = \min(\alpha_{DP} P, \alpha_{DS} S, \mu_D^m) \tag{32}$$

$$\mu_H = \min(Y_H \alpha_H B, \mu_H^m) \tag{33}$$

$$\mu_C = \min(Y_C \alpha_C (H+A), \mu_C^m) \tag{34}$$

$$\mu_m = \min(Y_M \alpha_M (D+\sigma C), \mu_M^m) \tag{35}$$

Table 7
Periods with different types of modelled growth rate limitation for bacteria (B) and diatoms (D) in the different mesocosms

		Day 0	1	2	3	4	5	6	7	8	9	10
C_0	B											
	D											
C_1	B											
	D											
C_3	B											
	D											
C_{10}	B											
	D											
C_0Si	B											
	D											
C_1Si	B											
	D											
C_3Si	B											
	D											
$C_{10}Si$	B											
	D											
K	B											
	D											
KC_{10}	B											
	D											

C-limitation of bacterial growth rate indicated by hatched, Si-limitation of diatoms by dotted areas. P-limitation indicated by open areas both for diatoms and bacteria.

of the forcing variables (P_t and M) and the set of numerical values chosen for the physiological parameters.

Since, at steady state, bacteria cannot consume more BDOC than produced, $Y_{BC}\Psi$ defines a maximum steady state bacterial production. Following Thingstad (2003), this can be used to define a dimensionless "limitation index" η (Eq. (18)) that relates physiological and forcing parameters so that $\eta > 1$ and $\eta < 1$ correspond to steady states with carbon- and mineral-nutrient limited bacterial growth, respectively (Eq. (18)). For the values used here (Table 4), $\eta = 9.6$, and the initial state is thus characterised by a strong carbon-limitation of bacterial growth rate.

With diatoms present and all osmotrophs P-limited, steady state values for all state variables, except diatoms, in the microbial sub-system (i.e. P^*, B^*, A^*, H^*, and C^*) are independent of the total nutrient content P_t, but proportional to diatom loss rate, which again is proportional to mesozooplankton biomass ($\alpha_M M$). Diatom biomass (D^*) on the other hand decreases with M, but increases with P_t (Eq. (14)). High nutrient content in the microbial part will thus give high diatom biomass, while a high fraction of total biomass in mesozooplankton will give a low value for diatoms and high values for all the other state variables in the microbial part. With a sufficiently high ratio between biomass in higher predators and nutrient content of the microbial system, diatoms will disappear (Eq. (16)). This leads to a different steady state solution not discussed here.

The model also contains a selectivity coefficient σ for mesozooplankton predation on ciliates, allowing for a potential difference in mesozooplankton clearance rate of ciliates and diatoms. Increasing the selectivity σ for ciliates will increase the steady state concentration of autotrophic flagellates while diatom concentration
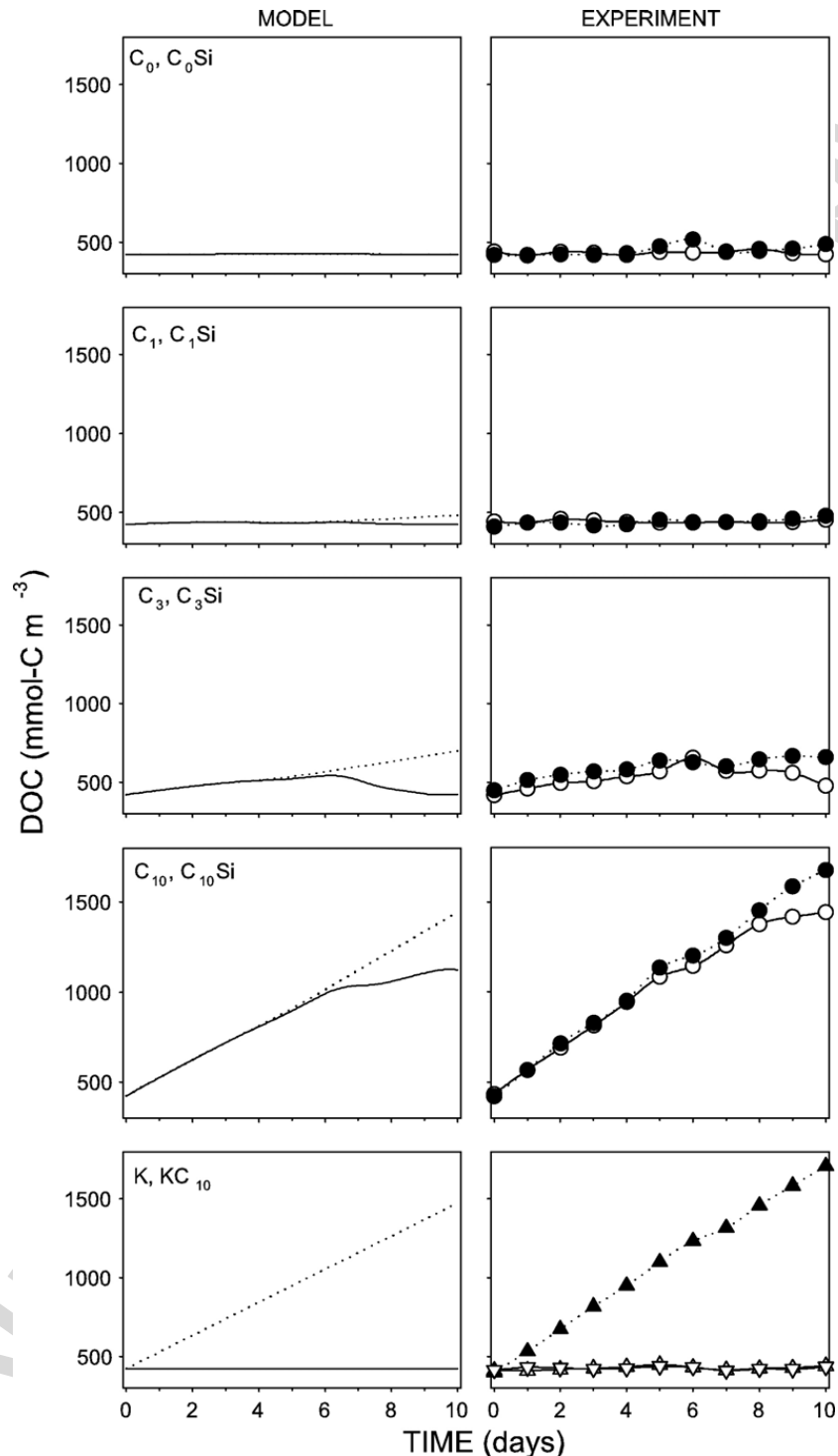

Fig. 2. Temporal changes in dissolved organic carbon (DOC) modelled (left column) and observed (right column). Mesocosms with 0, 1, 3 and 10× Redfield ratio between daily additions of glucose-C and mineral nutrient are shown in rows 1,2,3 and 4, respectively. Mesocosms without silicate added are marked with solid lines (model) or solid lines and open circles (observed). Mesocosms with silicate added are marked with dotted lines (model) or dotted lines and filled circles (observations). Control mesocosms K_a and K_b (solid line and solid line — open triangles for model and observations, respectively) and KC_{10} (dotted line, dotted line — filled triangles for model and observations, respectively) are shown in line 5. Same scale on y-axis for modelled and observed results. Observational data from Havskum et al. (2003).

decreases (Eqs. (13) and (14)). Changing σ will thus change the diatom:flagellate balance in the steady state phytoplankton community.

In this model, diatoms (when present) and autotrophic flagellates compete with bacteria, but also with each other, for the limiting mineral nutrient. Interestingly, this gives the somewhat counterintuitive net effect that mineral nutrient limited bacterial production BP_β^* increases proportionally to autotroph flagellate affinity (α_{AP}) when

diatoms are present. Diatom affinity (α_{DP}), however, exerts a strong negative effect through its squared inverse relationship to BP_β^* (Eq. (15)).

3. Simulating the response to mesocosm manipulations

The mesocosm manipulations used are summarised in Table 5 (see Havskum et al. (2003) for further details). In the experiment, nutrients were added as single daily
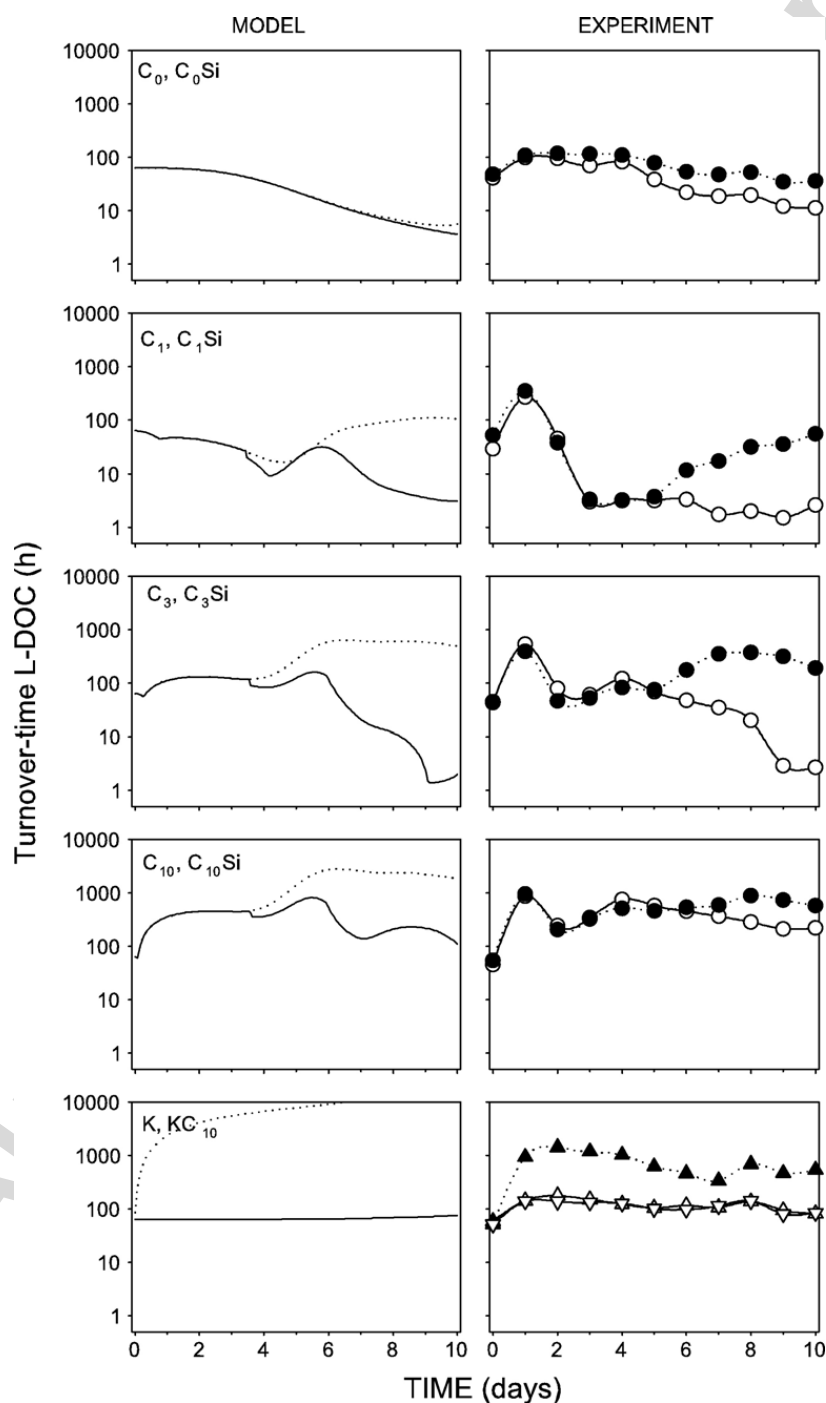

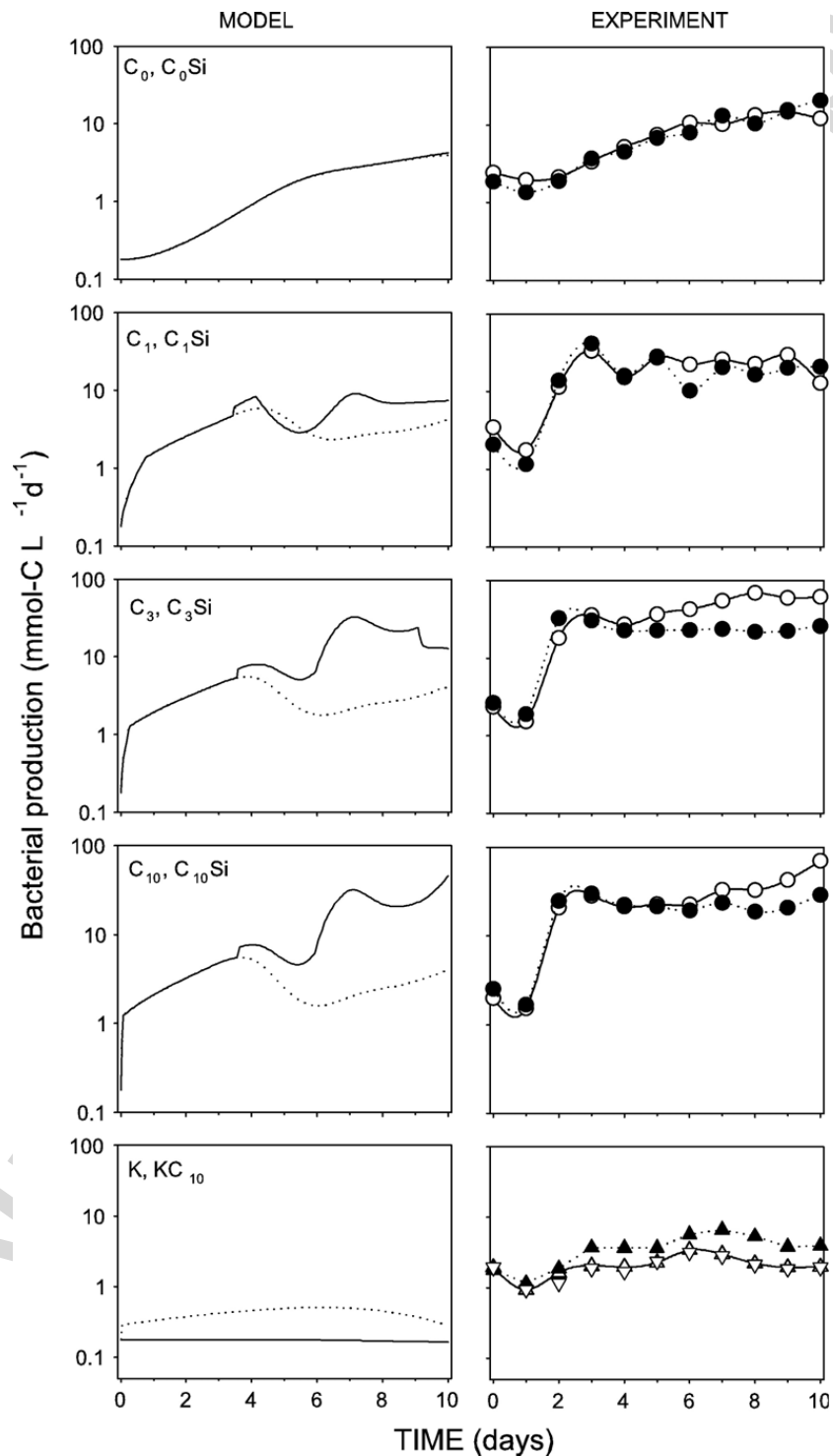Fig. 3. Turnover-time for glucose. Symbol use and arrangement of panels for modelled and observed results as in Fig. 2. Observational data from Havskum et al. (2003).

additions. The model has continuous additions giving an integrated daily addition equal to the experimental dose. There are no experimental data for the <24 h transients following nutrient additions, and adding all the complications of a Droop-type model with potential for reproduction of the short-dynamics was not felt warranted in this case.

Eight of the 10 mesocosms received nitrate and phosphate in Redfield ratio. These eight mesocosms were split in two gradients with increasing daily additions of glucose-C corresponding to 0, 1, 3 or 10 times the Redfield ratio (C:N:P=106:16:1 M) relative to the mineral nutrients added. These two gradients, parallel in their glucose addition, are

Fig. 4. Bacterial production. Symbol use and arrangement of panels for modelled and observed results as in Fig. 2. Observational data from Havskum et al. (2003).

subsequently called the C-series and the CSi-series, and differ only in their silicate addition.

In the C-series, the naturally occurring free silicate was depleted between day 3 and day 4, while in the CSi-series, silicate was kept replete by daily Si-additions from day 3 (from 84 h in the model). Both in the model and in the experiments, the pairs C_0–C_0Si, C_1–C_1Si, C_3–C_3Si and C_{10}–$C_{10}Si$ are thus parallels for the first 3 d of the experiment. The dynamic behaviour of the food web model was described with the differential equations in Table 6, built on the same growth and loss terms as the steady state equations in Table 1, but differing in the inclusion of a
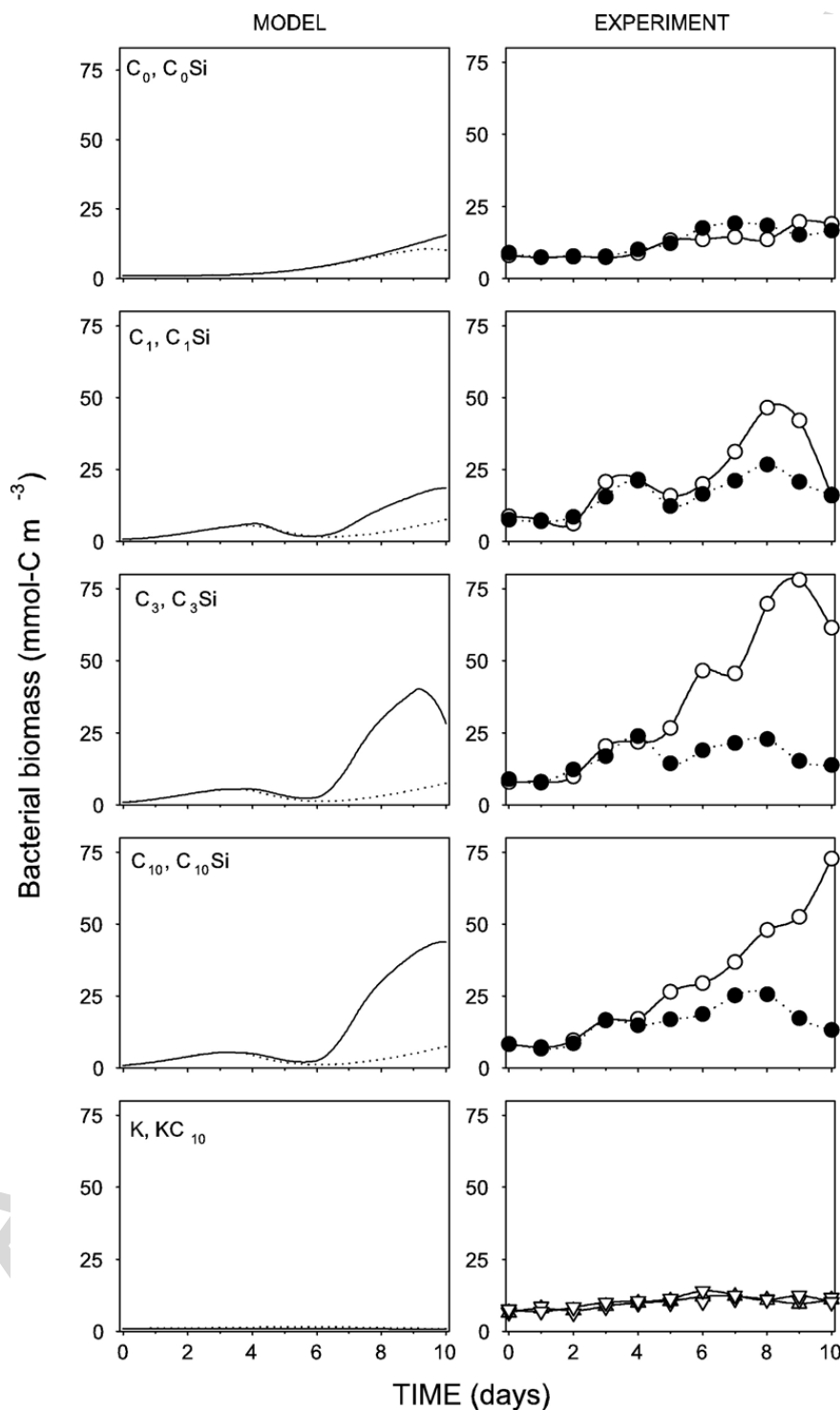

Fig. 5. Bacterial biomass. Symbol use and arrangement of panels for modelled and observed results as in Fig. 2. Observational data from Havskum et al. (2003).

maximum specific growth rate for all organism groups. In the C_0–C_0Si pair where no allochthonous C-source was added, bacterial production was observed to increase in very close proportionality to the square of total-P. In this version of the model we therefore used the empirical relationship $\Psi = k(P_t + M)^2$ for the production rate Ψ for BDOC (L) and total-P ($P_t + M$) in the system (Eq. (28)). A background pool of 420 mmol-C m^{-3} recalcitrant DOC is assumed, not influencing the dynamics of the model, but allowing us to present measured and simulated DOC values on the same scale.

Conversion from P-units to C-units in biomass is done assuming fixed stoichiometry (molar C:P = 50 in bacteria, 106 otherwise).

The equations were solved numerically using the Berkeley Madonna® programme with a 4th order Runge–Kutta routine and a fixed time-step of 0.01 h.

3.1. Temporal shifts in limitation

Central to the dynamics of the model are the shifts occurring between limiting factors for bacteria and diatoms. For the bacteria, the shifts are between phosphate and carbon limitation, and between phosphate and silicate limitation in diatoms (Table 1). Phosphate addition initiates diatom growth in the model, thereby depleting the initially present silicate around day 3.5–4.5 in the C-gradient, reproducing well the silicate depletion observed experimentally (Havskum et al., 2003). In the CSi-gradient, silicate addition prevents Si-limitation. The initial C-limitation of bacteria remains throughout the simulated period in C_0, C_0Si and K. In C_1, the added glucose is consumed after ca. 4 d and the bacteria return to C-limitation. In C_3, the return to C-limitation is delayed until day 9, while the system does not, during the duration of the experiment, build up a sufficient potential for depletion of the glucose added to the C_{10} mesocosm. In the Si gradient, the competition from diatoms prevents the depletion of the added glucose and a return to C-limitation within the experimental period. The molar stoichiometric coefficient for phosphorous:silicate (ρ_{DS}) had to be given a somewhat low value (0.04) in order to get a correct timing for silicate depletion in the modelled C-series, but may be realistic for diatoms having access to surplus Si in this period.

3.2. Dissolved organic carbon concentration and turnover-time

The pattern in limitation shifts described in Table 7 is reflected in the modelled DOC dynamics (Fig. 2). In the mesocosms the added glucose was consumed to a larger extent in the C_1, C_3, and C_{10} mesocosms, than in the corresponding C_1Si, C_3Si, and C_{10}Si mesocosms where strong competition from Si-replete diatoms remain throughout the experimental period. The pattern modelled for DOC corresponds closely to the pattern observed. In both model and experiment, DOC in C_3, but not in C_3Si, returns to background level towards the end of the experiment. Also, the increasing difference between observed DOC levels in C_{10} and C_{10}Si is well represented by the model. The increase with time in the ability of the ecosystem in the modelled C-series to consume glucose is caused by the transfer of added mineral nutrients up the food chain to the predator level, whereby biomass of algal nutrient competitors is reduced, and regeneration of mineral nutrients increases (cf. Eq. (15) for the steady state situation). Due to the slow transfer in the diatom–mesozooplankton link, nutrients are immobilized in diatom biomass in the modelled CSi-series, preventing any corresponding increase in the ability of the model's now P-limited bacteria to degrade the added glucose. Due to a high background level of recalcitrant DOC, small variations in DOC as modelled in e.g. C_1 and C_1Si, were difficult to observe experimentally (Figs. 2 and 3).

Turnover-time $T = L/V$, where L is concentration and V is the consumption rate for BDOC, should be a sensitive indicator of shifts in bacterial limitation. A shift to P-limitation will reduce V. With supply rate remaining unaffected, L will then increase, and T would be expected to increase strongly due to the combined effect on increasing numerator and decreasing denominator. The modelled pattern for turnover-time of BDOC corresponds well with the observed turnover-time for glucose (Fig. 3) and both model and observations exhibit a split in turnover-time between all the pairs C_1–C_1Si, C_3–C_3Si and C_{10}–C_{10}Si, following the onset of Si-addition to the CSi-series.

3.3. Bacterial production

With an initial C-limited state for the bacteria, bacteria respond to glucose addition in the model with an immediate shift-up in growth rate, and thus in bacterial production. An abrupt shift-up was also observed in the experimental system, although here the response was delayed to day 2. With an ability to reproduce the shift-up, the increasing trend in mesocosms receiving mineral nutrients only (C_0, C_0Si), and the negative effect of Si, we consider the model's ability to reproduce the observed pattern of changes in bacterial production to be good. Note however that bacterial

production in the initial state, in mesocosms supplied with mineral nutrients, but not with glucose (C_0 and C_0Si), and in the control (K), is about one order of magnitude lower in the model than in the observations. In the model, bacteria in these mesocosms remain C-limited throughout the simulated period and bacterial production is therefore directly proportional to the system's production (Ψ) of BDOC (bacterial yield Y_{BC} is a constant in the model). We could easily adjust parameters to fit the level of bacterial production, but found no way to do this without a simultaneous deterioration, either of the simulated patterns of bacterial production, or in the model's performance in other respects (see Discussion for further details) (Fig. 4).
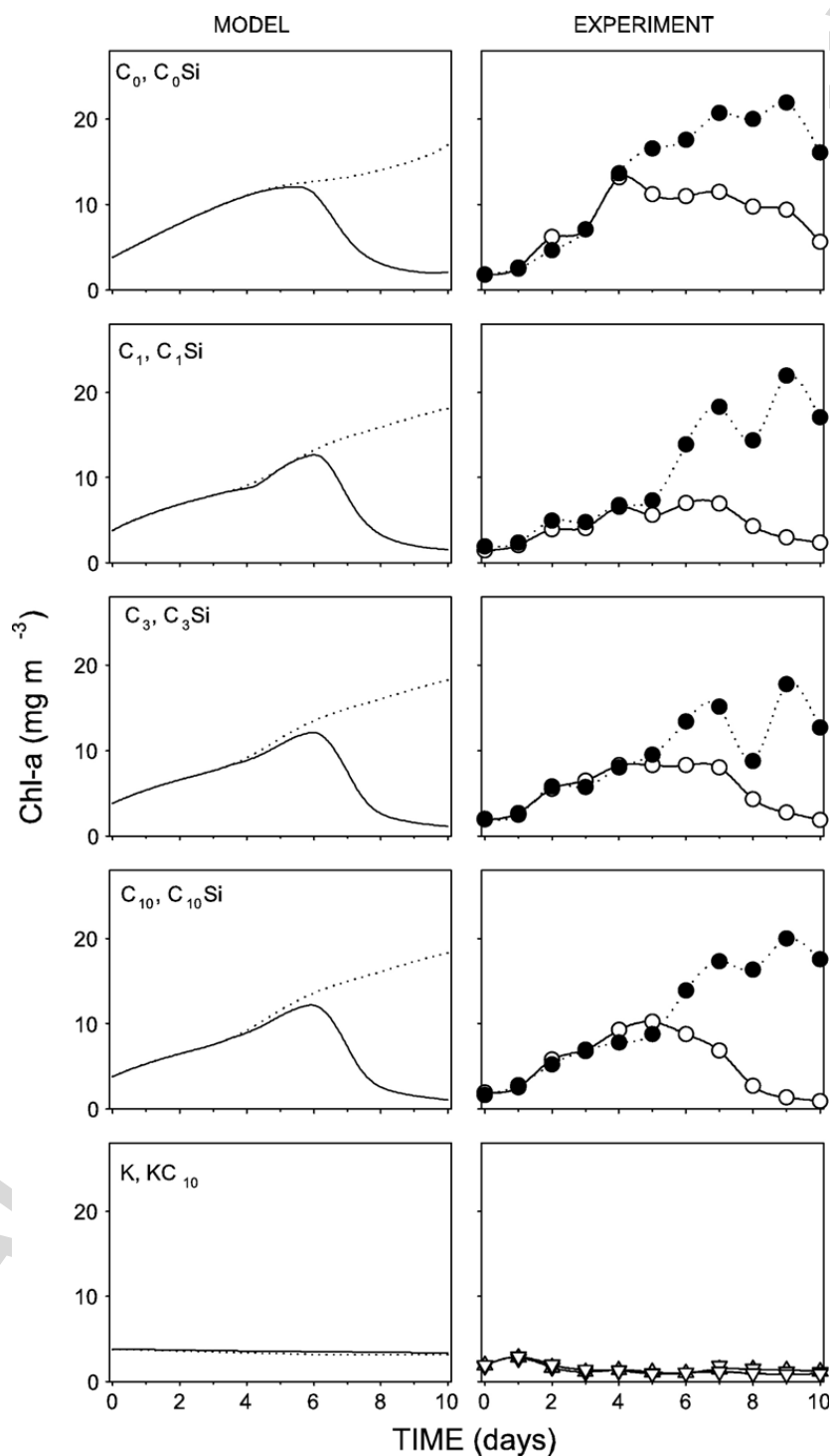

Fig. 6. Chlorophyll—a. Symbol use and arrangement of panels for modelled and observed results as in Fig. 2. Observational data from Havskum et al. (2003).

3.4. Bacterial biomass

When both mineral nutrients and glucose are added, the model produces predator–prey oscillations in the bacteria–heterotrophic flagellate system. Such oscillations are also visible in the observed bacterial biomass. Bacterial biomass tends to be slightly lower in the model than in the observations. Bacterial biomass level in the model is particularly sensitive to yield (Y_H) and clearance rate (α_H) of heterotrophic flagellates (cf. Eq. (9)); lowering of any of these would increase the modelled bacterial biomass. In accordance with reported values (Fagerbakke et al., 1996), we have used a lower C:P ratio in bacteria ($\rho_B = 50$, M), than in other biomass (106). Removing this difference would obviously also increase bacterial C-biomass (Fig. 5).
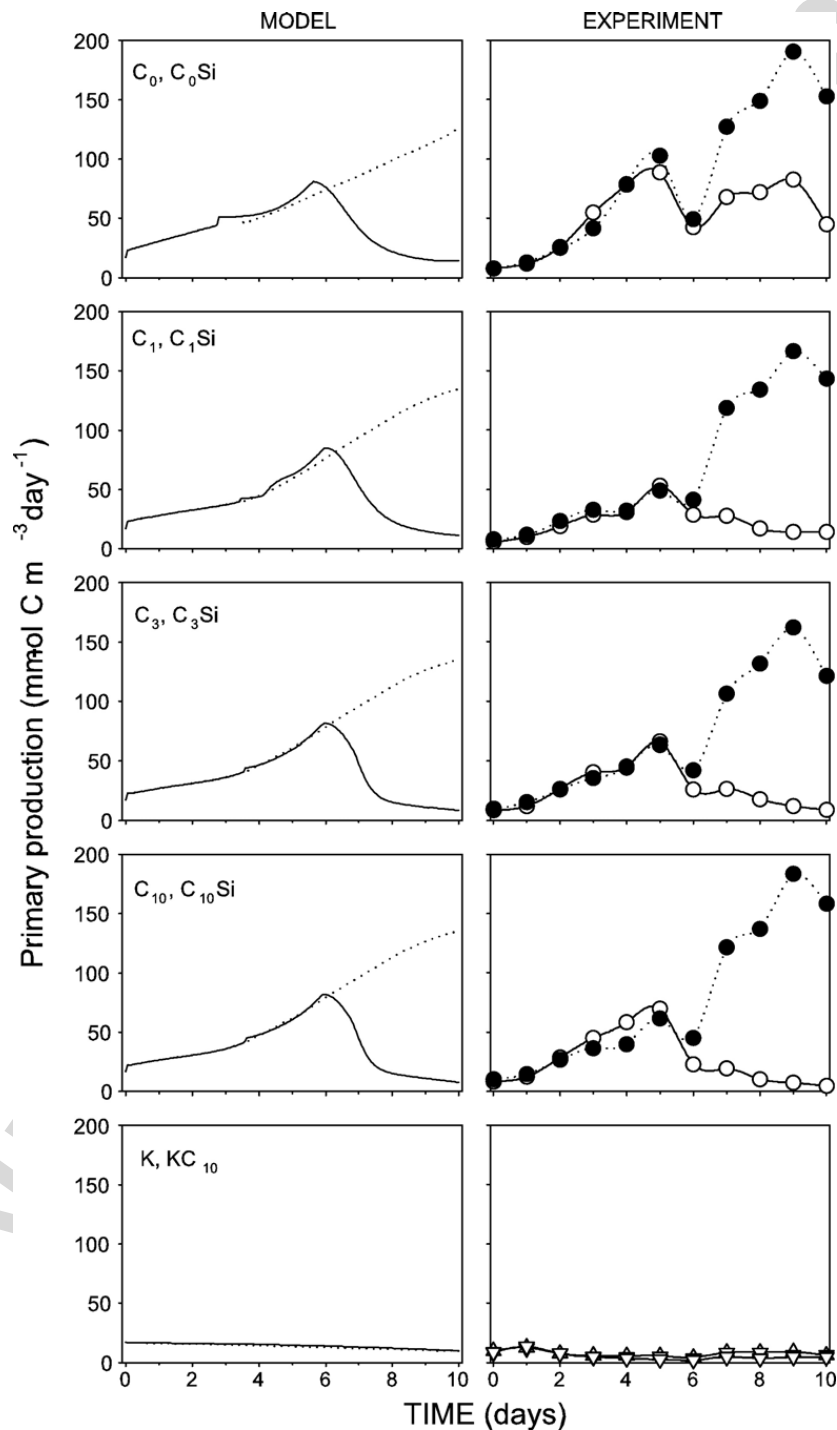

Fig. 7. Primary production. Symbol use and arrangement of panels for modelled and observed results as in Fig. 2. Observational data from Havskum et al. (2003).
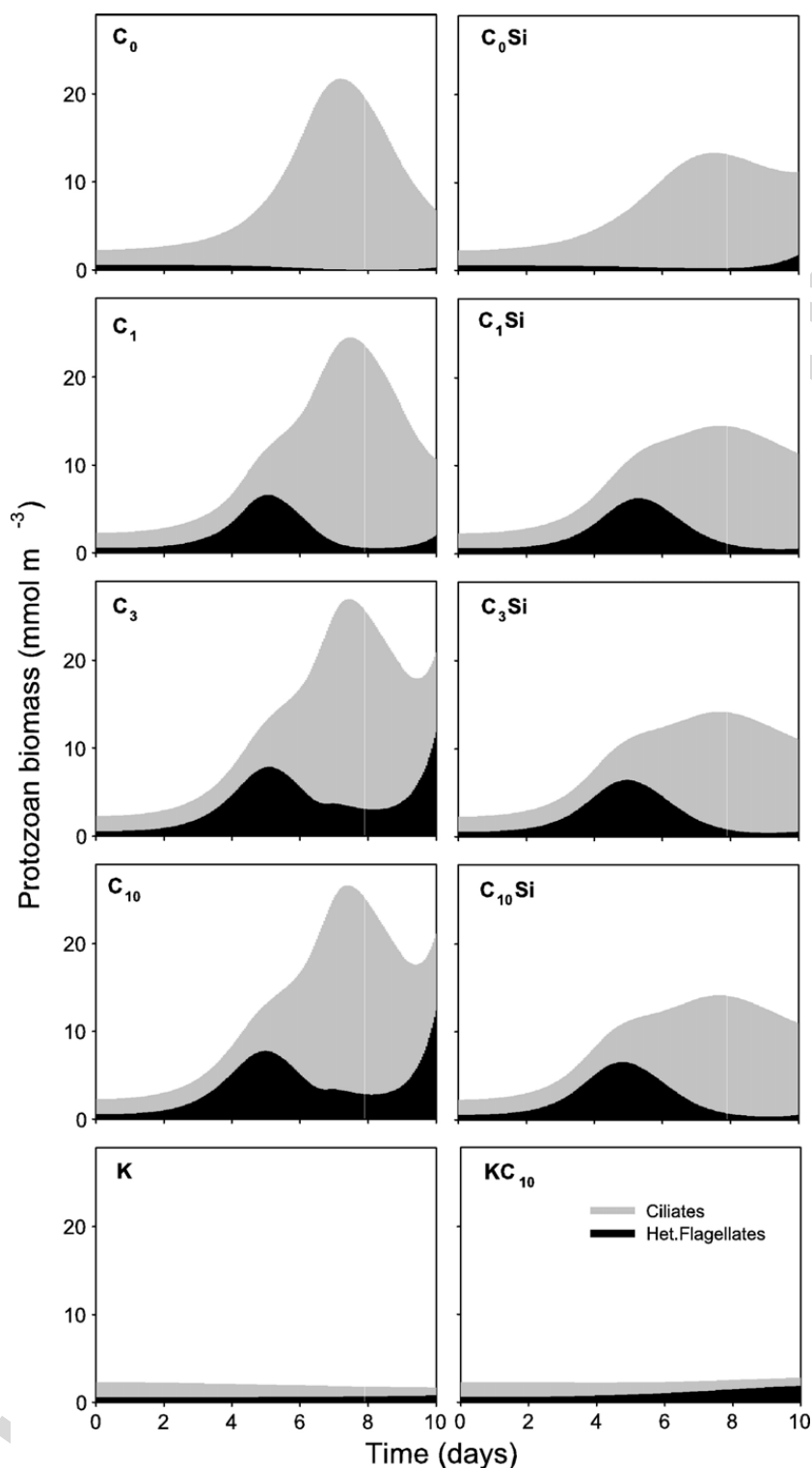
Fig. 8. Modelled heterotrophic flagellate (black) and ciliate (grey). Biomass represented as stacked area plots (upper limit of shaded area represents total protozoan biomass). Panels in line 1, 2, 3 and 4 correspond to glucose-C additions of 0, 1, 3 and 10× Redfield of daily mineral nutrient additions, respectively. Mesocosms without and with silicate additions in left and right columns, respectively. Control mesocosms in line 5 with K in left and KC_{10} in right column.

3.5. Chlorophyll and primary production

For both model and observations, the addition of silicate to the CSi-series leads to a split in chlorophyll levels with build-up of high chlorophyll levels in CSi-series, while chlorophyll in the C-series peaks in the middle of the experimental period. The reduction one might expect in chl in mesocosms where competition
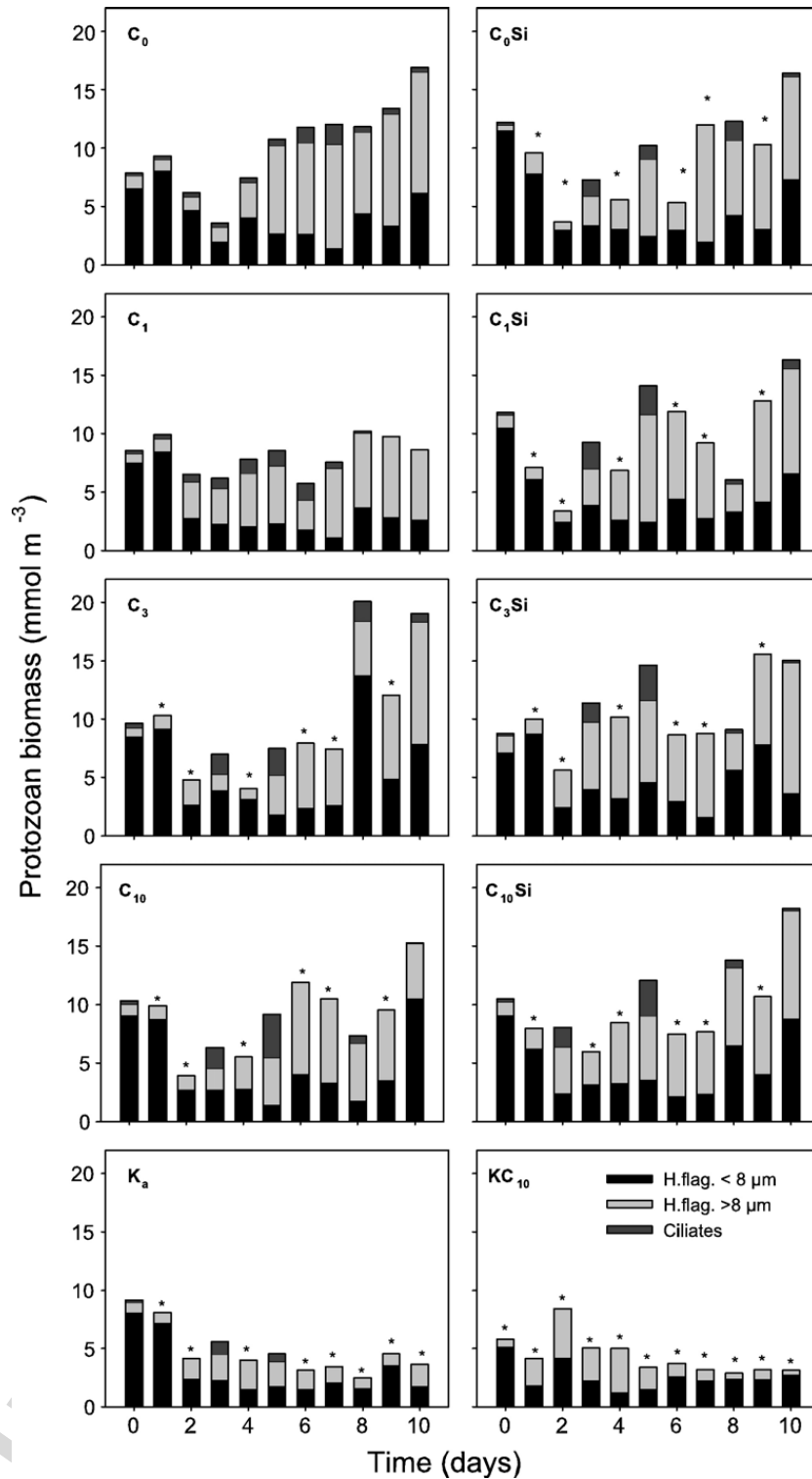
Fig. 9. Protozoan biomass, observed results, stacked bars with smallest size-fraction of heterotrophic flagellates at the bottom, ciliates on top. Panels arranged as in Fig. 8. Stars indicate samples where ciliate biomass was not determined. Observational data from Havskum et al. (2003).

from bacteria is stimulated by glucose is moderate, both in experiments and in model (Figs. 6 and 7).

In the CSi mesocosms, where the model produces a state with most of the added limiting nutrients immobi-

lized in high diatom biomass, a model assuming a fixed stoichiometry between P-uptake and C-fixation would produce very little diatom primary production. Running the model with such fixed stoichiometry (simulations not

shown) actually gave little difference in primary production between corresponding mesocosms in the C and CSi series. To be able to simulate the observed differences in primary production between the C and the CSi series of mesocosms, we found it necessary to include the potential for a C-overflow mechanism in primary production. This was done by calculating diatom carbon fixation (PP_D) from diatom biomass (D) and growth rate (μ_D) according to the equation $PP_D = \rho_A(\mu_D D + (1-\varepsilon)(\mu_D^{\max} - \mu_D)D)$, where ε represents the ability of nutrient limited phytoplankton to turn off the part of their photosynthetic capacity not being stoichiometrically coupled to growth. The model runs shown (Fig. 7) are done using the extreme case with $\varepsilon = 0$ for diatoms (C-fixation continues unaffected by mineral nutrient limitation) and $\varepsilon = 1$ (no C-overflow) in the corresponding expression for autotrophic flagellates, and reproduces in a reasonable manner both the pattern and the level of observed primary production.

3.6. The protozoa

When bacterial growth rate is C-limited, the steady-state effect in the model is a shift in biomass from heterotrophic to autotrophic flagellates (Eq. (8) combined with Eq. (11)), relative to the situation when bacteria are mineral nutrient limited. With a low bacterial production modelled in mesocosms without glucose addition (K, C_0, C_0Si), modelled biomass of heterotrophic flagellates is therefore low, and the model's main response to an addition of glucose alone (KC_{10}) is an increase in biomass of heterotrophic flagellates. Adding only mineral nutrients (C_0) gives a model response in autotrophic flagellates and a subsequent succession of ciliates. If Si is kept replete (C_0Si), modelled phytoplankton response is shifted from those that serve as ciliate prey (autotrophic flagellates) towards those that are not (diatoms), and the ciliate response is therefore reduced. When bacterial C-limitation is released by glucose addition, the response in heterotrophic flagellate biomass increases (C_1, C_3 and C_{10} compared to C_0), while competition from Si-replete diatoms reduces this effect (C_1Si, C_3Si and $C_{10}Si$ compared to C_1, C_3 and C_{10}, respectively) (Figs. 8 and 9).

Experimental data are available on biomass estimates of microscopically observed ciliates, and on colourless flagellates in different size-classes (Havskum et al., 2003). There is no direct way to compare these data to the model's two functional groups of "those that eat bacteria" (termed heterotrophic flagellates in the model) and "those that eat flagellates" (termed ciliates). Tentatively, flagellate data are here grouped in <8 μm and >8 μm cells as a somewhat arbitrary classification hoped to separate to

some extent between bacterial predators on one side, and predators on small phytoplankton and the bacterial predators on the other. Apart from a higher protozoan biomass in mesocosms with mineral nutrients added (C- and CSi-series) than in controls without (K and KC_{10}), we found, however, few convincing trends in the observed response patterns of protozoa (Fig. 9).

3.7. Mesozooplankton

The initial value used for the model's mesozooplankton compartment $M = 40$ μmol-P m^{-3} may seem high when compared to a total initial phosphorous content of $P_t = 220$ μmol-P m^{-3} in the microbial part of the food web. Converted to biomass-C with a C:P = 106:1 M Redfield ratio, modelled mesozooplankton biomass level is however in general agreement with the observed level of mesozooplankton as collected in the >37 μm size fraction
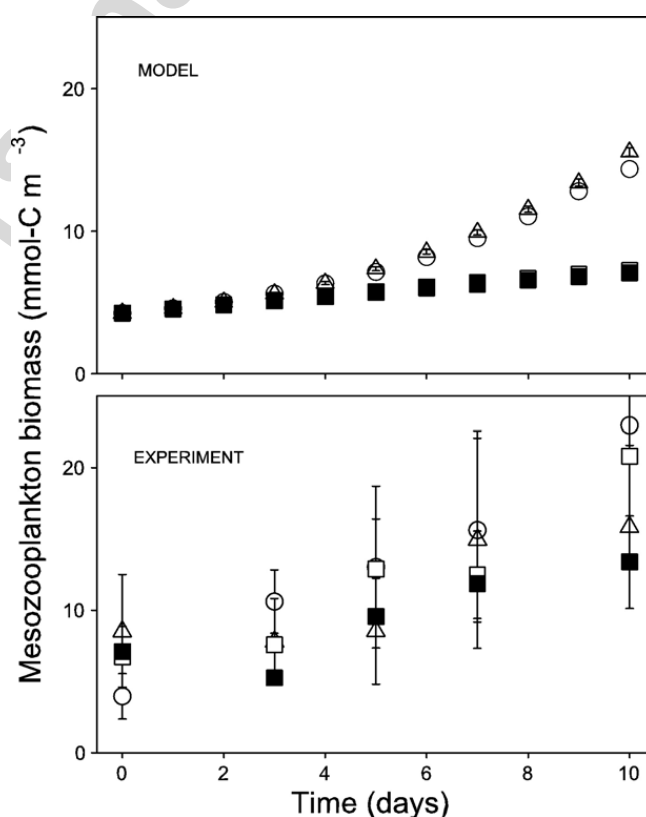

Fig. 10. Modelled mesozooplankton biomass (upper panel) and observed mesozooplankton abundance (lower panel). Open circles with error bars represent mean and standard deviation for mesocosms in gradient C_0–C_{10}, open triangles with error bars represent mean and standard deviation for mesocosms in gradient C_0Si–$C_{10}Si$, open and filled squares represent K, and KC_{10} mesocosms, respectively. Note that error bars for modelled results (upper panel) represent differences between treatments, in the case of observations (lower panel) they represent the sum of variation due to differences between treatments and measurement errors. Observational data from Havskum et al. (2003).

(Havskum et al., 2003). With its squared effect on η (Eq. (18)), high mesozooplankton biomass M is a strong factor in forcing the initial state of the model towards C-limited bacterial growth. A high mesozooplankton biomass may thus be a clue to why this Danish fjord ecosystem apparently had C-limited bacteria. Adding mineral nutrients leads to a succession, either via ciliates or via diatoms, to mesozooplankton, and thus to an increase with time in modelled mesozooplankton biomass in both the C- and the CSi-series. Neither the differences in organic-C supply along the C- and CSi-series, nor the difference in diatom dominance between the C- and CSi-series, lead to large differences in the modelled mesozooplankton biomass (Fig. 10d). As for microzooplankton, a large uncertainty in the observational data, combined with uncertainties related to the correspondence between observed species and the models simple functional group of "mesozooplankton", makes it difficult to make rigorous comparisons between model and observational data (Fig. 10).

4. Discussion

Accumulation of DOC in the photic zone is currently believed to be a core process in the oceanic C-cycle (Hansell, 2002). Since accumulation is the net result of production, consumption, and export, proper understanding of all three mechanisms is a prerequisite for the construction of models capable of representing the present C-cycle and its potential response to climate change. The work presented here primarily focuses on the consumption aspect by exploring the extent to which we could model the consumption of allochthonous, easily bioavailable DOC, added as glucose in the experimental work. The fundamental hypothesis explored here is that control of such consumption is closely linked to whether bacterial growth is limited by mineral nutrients or by organic-C.

In order to represent the modifying effects of glucose and Si additions on the flow of phosphorous through the food web, a minimum of three osmotroph populations seems to be required. To allow for steady states with all three osmotroph populations coexisting on the same limiting nutrient (free phosphate), we need the two selective protozoan predators. In order to get a dynamically changing transfer of the limiting element out of the microbial part of the food web, we also need mesozooplankton as a dynamic variable. The food web structure in Fig. 1 therefore seems to be as close to our ideal of a minimum model as we could get for a natural system believed to contain a vast amount of trophic interactions, physiological mechanisms, and biological diversity. The model has two elements in the stoichiometric coupling deviating from our "simplest possible" ideal. Bacteria

were, based on literature values, given a C:P-stoichiometry of 50 (molar), instead of the Redfield value of 106 used for all other organisms. Also, based on mesocosm observations and literature data, diatom C-fixation was assumed to have a C-overflow mechanism (Engel et al., 2004) that assumed C-fixation to run independently of diatom growth rate limitation. This allows continued C-fixation in model states where mineral nutrients were immobilized in diatom biomass and was vital to get a correct simulation of the effect of Si on primary production. Increased levels of organic-C in diatom-dominated communities is well documented experimentally (Egge and Jacobsen, 1997; Engel et al., 2002). Although diverting from our ideal of a "simplest possible" model, the inclusion of a diatom-specific mechanism increasing the ratio between C-fixation and mineral nutrients assimilated, thus seems easily justified.

This simple model was exposed to what we consider a rather demanding challenge: We wanted one single flow structure, with one single set of parameters, to reproduce not only a steady state comparable to the observed, but also to reproduce the dynamic transients resulting from 9 different experimental perturbations, all starting from the same steady state.

In this perspective, we found it quite satisfactory that the model had enough elements to reproduce well the observed variations in DOC and the turnover-time for BDOC, meaning that the added glucose was consumed in reasonably correct amounts at reasonably correct times in the model. Central for the model's ability to do so is an ability to reproduce the timing in shifts in limitation states such as illustrated in Table 7. The model also produces, not only a qualitatively correct, but also quantitatively reasonably accurate effects of Si on most of the observed variables (see Figs. 2, 5, 6 and 10).

The major problem we could identify for this "minimum" model to reproduce the observations was for bacterial production. The parameter set used does a reasonable job in reproducing the level of bacterial production late in the experiment in glucose-amended bags, and also reproduces the early phenomenon of an abrupt shift-up in bacterial production in glucose-amended mesocosms. In the model, this abrupt shift-up is caused by the sudden release of C-limitation as glucose is added, and thus requires a parameter set that gives a steady state characterized by limitation index (see Eq. (18)) $\eta \gg 1$. It is easy to give the model a correct level of bacterial production in the control bag by increasing the production rate Ψ (e.g. by increasing the parameter k by a factor of ~ 10). However; to retain the pattern with an initial shift-up in bacterial

production, either other parameters, or mesozooplankton biomass (M) would then need to be changed subject to the constraint that the expression (from Eq. (18)) $\eta = Y_{BC}^{-1} Y_H^{-1} \frac{\alpha_{BP} \alpha_{AP}}{\alpha_H \alpha_{DP}^2} \frac{\alpha_M^2}{\Psi} M^2$ must remain $\gg 1$, signifying a strongly C-limited bacterial growth rate. We have not been able to change the model in this manner without seriously deteriorating its performance in other respects. Although we cannot from this exclude that such a parameter set exists, we suspect that some of the explanation for this problem lies in the profound biological effects of glucose observed by Havskum et al. (2003) on the bacterial community. If one combines the idea that glucose addition forces bacteria to mineral nutrient limitation, with the prevalent idea that small organisms are superior competitors for mineral nutrients, one would tend to expect glucose to favour the selection of small bacteria. Contrary to this theoretical line of argument, glucose addition was found to lead to a bacterial community dominated by large "sausage"-formed bacteria. Similarly Malits et al. (2004) also found that when the addition of organic carbon was unbalanced with respect to inorganic nutrients, bacteria grew larger. Thingstad et al. (2005b) have recently argued that this may be a special version of a strategy whereby some osmotroph micro-organisms use a non-limiting substrate (here glucose) to simultaneously increase nutrient affinity and reduce predation. If such an interpretation is correct, the addition of glucose would change bacterial affinity (α_B), heterotrophic flagellate clearance rate (α_H), as well as bacterial yield (Y_{BC}), and possibly the yield (Y_H) of heterotrophic flagellates, thus changing the value of η (Eq. (18)). This would have profound effects on both the steady state and the dynamics of transient responses, and we suspect that either a change of the flow structure by introducing an extra bacterial population, and/or a change to a much more flexible physiological control of bacterial parameters, may be necessary in order to reproduce observed bacterial production under both C- and mineral nutrient limiting conditions. Such additions would make the model much more complicated and less transparent, and have so far not been explored further.

Sharing the view that addition of complexity and detail to present plankton models needs to be done in small and well-understood steps (Anderson, 2005) we feel that understanding the behaviour of "simplest possible" models is a required step before adding more sophisticated biological detail. In light of this we feel the ability of the model to quantitatively reproduce so much of our experiment to be very encouraging, supporting the idea that its flow structure captures a central set of the control mechanisms in the lower part of the pelagic food web. The conclusion that more sophisticated biological detail need to be included in models when trying to reproduce dynamic responses following from drastic shifts in limitation, is in accordance with recent experience from other nutrient manipulation experiments (Thingstad et al., 2005a).

Acknowledgements

References

Anderson, T.R., 2005. Plankton functional type modelling: running before we can walk? J. Plankton Res. 27 (11), 1073–1081.

Azam, F., Fenchel, T., Field, J.G., Gray, J.S., Meyer-Reil, L.A., Thingstad, T.F., 1983. The ecological role of water-column microbes in the sea. Mar. Ecol., Prog. Ser. 10, 257–263.

Baretta-Bekker, J.G., Baretta, J.W., Koch Rasmussen, E., 1995. The microbial food web in the european regional seas ecosystem model. Neth. J. Sea Res. 33, 363–379.

Baretta-Bekker, J.G., Baretta, J.W., Ebenhoh, W., 1997. Microbial dynamics in the marine ecosystem model ERSEM II with decoupled carbon assimilation and nutrient uptake. J. Sea Res. 38, 195–211.

Billen, G., Servais, P., 1989. Modélisation des processus de dégradation bactérienne de la matière organique en milieu aquatique. In: Bianchi, M., Maty, D., Bertrand, J.-C., Caumette, P., Gauthier, M. (Eds.), Micro-organismes dans les écosystèmes océaniques. Masson, Paris, pp. 219–241.

Egge, J.K., Jacobsen, A., 1997. Influence of silicate on particulate carbon production in phytoplankton. Mar. Ecol., Prog. Ser. 147 (1–3), 219–230.

Engel, A., Goldthwait, S., Passow, U., Alldredge, A., 2002. Temporal decoupling of carbon and nitrogen dynamics in a mesocosm diatom bloom. Limnol. Oceanogr. 47 (3), 753–761.

Engel, A., Delille, B., Jacquet, S., Riebesell, U., Rochelle-Newall, E., Terbrüggen, A., Zondervan, I., 2004. Transparent exopolymer particles and dissolved organic carbon production by *Emiliania huxleyi* exposed to different CO_2 concentrations: a mesocosm experiment. Aquat. Microb. Ecol. 34, 93–104.

Fagerbakke, K., Heldal, M., Norland, S., 1996. Content of carbon, nitrogen, oxygen, sulfur and phosphorus in native aquatic and cultured bacteria. Aquat. Microb. Ecol. 10, 15–27.

Fasham, M.J.R., Ducklow, H.W., McKelvie, S.M., 1990. A nitrogen-based model of plankton dynamics in the oceanic mixed layer. J. Mar. Res. 48 (3), 591–639.

Hansell, D.A., 2002. DOC in the global ocean carbon cycle. In: Hansell, D.A., Carlson, C.A. (Eds.), Biogeochemsitry of Marine Dissolved Organic Matter. Academic Press, pp. 685–711.

Harrison, W.G., Azam, F., Renger, E.H., Eppley, R.W., 1977. Some experiments on phosphate assimilation by coastal marine plankton. Mar. Biol. 40, 9–18.

Havskum, H., Thingstad, T.F., Scharek, R., Peters, F., Berdalet, E., Sala, M.M., Alcaraz, M., Bangsholt, J.C., Zweifel, U.L., Hagstrom, A., Perez, M., Dolan, J.R., 2003. Silicate and labile DOC interfere in structuring the microbial food web via algal–bacterial

competition for mineral nutrients: results of a mesocosm experiment. Limnol. Oceanogr. 48 (1), 129–140.

Jacquet, S., Havskum, H., Thingstad, T., Vaulot, D., 2002. Effects of inorganic and organic nutrient addition on a coastal microbial community (Isefjord, Denmark). Mar. Ecol., Prog. Ser. 228, 3–14.

Kirchman, D., 1994. The uptake of inorganic nutrients by heterotrophic bacteria. Microb. Ecol. 28, 255–271.

Malits, A., Peters, F., Bayer-Giraldi, M., Marrase, C., Zoppini, A., Guadayol, O., Alcaraz, M., 2004. Effects of small-scale turbulence on bacteria: a matter of size. Microb. Ecol. 48 (3), 287–299.

Moloney, C.L., Field, J.G., 1991. The size-based dynamics of plankton food webs. 1. A simulation model of carbon and nitrogen flows. J. Plankton Res. 13, 1003–1038.

Pomeroy, L.R., 1974. The ocean's food web: a changing paradigm. Bioscience 24, 499–504.

Pomeroy, L.R., Sheldon, J.E., Sheldon, W.M.J., Peters, F., 1995. Limits to growth and respiration of bacterioplankton in the Gulf of Mexico. Mar. Ecol., Prog. Ser. 117, 259–268.

Rigler, F.H., 1956. A tracer study of the phosphorous cycle in lake water. Ecology 37, 550–562.

Rivkin, R., Anderson, M., 1997. Inorganic nutrient limitation of oceanic bacterioplankton. Limnol. Oceanogr. 42, 730–740.

Sala, M.M., Peters, F., Gasol, J.M., Pedros-Alio, C., Marrase, C., Vaque, D., 2002. Seasonal and spatial variations in the nutrient limitation of bacterioplankton growth in the northwestern Mediterranean. Aquat. Microb. Ecol. 27 (1), 47–56.

Suttle, C., Fuhrman, J., Capone, D., 1990. Rapid ammonium cycling and concentration-dependent partitioning of ammonium and phosphate: implications for carbon transfer in planktonic communities. Limnol. Oceanogr. 35, 424–433.

Taylor, A.H., Joint, I., 1990. A steady-state analysis of the 'microbial loop' in stratified systems. Mar. Ecol., Prog. Ser. 59, 1–17.

Thingstad, T.F., 2003. Physiological models in the context of microbial food webs. In: Findlay, S., Sinsabaugh, R.L. (Eds.), Aquatic Ecosystems. Interactivity of Dissolved Organic Matter. Aquatic Ecology. Academic Press, pp. 383–395.

Thingstad, T.F., Lignell, R., 1997. Theoretical models for the control of bacterial growth rate, abundance, diversity and carbon demand. Aquat. Microb. Ecol. 13 (1), 19–27.

Thingstad, T.F., Pengerud, B., 1985. Fate and effect of allochthonous organic material in aquatic microbial ecosystems. An analysis based on chemostat theory. Mar. Ecol., Prog. Ser. 21, 47–62.

Thingstad, T., Rassoulzadegan, F., 1999. Conceptual models for the biogeochemical role of the photic zone food web, with particular reference to the Mediterranean Sea. Prog. Oceanogr. 44, 271–286.

Thingstad, T.F., Hagstrom, A., Rassoulzadegan, F., 1997. Accumulation of degradable DOC in surface waters: is it caused by a malfunctioning microbial loop? Limnol. Oceanogr. 42 (2), 398–404.

Thingstad, T.F., Havskum, H., Kaas, H., Nielsen, T.G., Riemann, B., Lefevre, D., Williams, P.J.l.B., 1999a. Bacteria–protist interactions and organic matter degradation under P-limited conditions: analysis of an enclosure experiment using a simple model. Limnol. Oceanogr. 44 (1), 62–79.

Thingstad, T.F., Perez, M., Pelegri, S., Dolan, J., Rassoulzadegan, F., 1999b. Trophic control of bacterial growth in microcosms containing a natural community from northwest Mediterranean surface waters. Aquat. Microb. Ecol. 18 (2), 145–156.

Thingstad, T.F., Krom, M.D., Mantoura, R.F.C., Flaten, G.A.F., Groom, S., Herut, B., Kress, N., Law, C.S., Pasternak, A., Pitta, P., Psarra, S., Rassoulzadegan, F., Tanaka, T., Tselepides, A., Wassmann, P., Woodward, E.M.S., Riser, C.W., Zodiatis, G., Zohary, T., 2005a. Nature of phosphorus limitation in the ultraoligotrophic eastern Mediterranean. Science 309 (5737), 1068–1071.

Thingstad, T.F., Øvreås, L., Løvdal, T., Heldal, M., 2005b. Use of non-limiting substrates to increase size; a generic strategy to simultaneously optimize uptake and minimize predation in pelagic osmotrophs? Ecol. Lett. 8, 675–682.

Vallino, J.J., Hopkinson, C.S., Hobbie, J.E., 1996. Modeling bacterial utilization of dissolved organic matter: optimization replaces Monod growth kinetics. Limnol. Oceanogr. 41 (8), 1591–1609.

Van den Meersche, K., Middelburg, J.J., Soetaert, K., van Rijswijk, P., Boschker, H.T.S., Heip, C.H.R., 2004. Carbon–nitrogen coupling and algal–bacterial interactions during an experimental bloom: modeling a C-13 tracer experiment. Limnol. Oceanogr. 49 (3), 862–878.

Van Wambeke, F., Christaki, U., Giannokourou, A., Moutin, T., Souvemerzoglou, K., 2002. Longitudinal and vertical trends of bacterial limitation by phosphorus and carbon in the Mediterranean Sea. Microb. Ecol. 43 (1), 119–133.

Wheeler, P.A., Kirchman, D.L., 1986. Utilization of inorganic and organic nitrogen by bacteria in marine systems. Limnol. Oceanogr. 31, 998–1009.

Williams, P.J.L., 1981. Incorporation of microheterotrophic processes into the classical paradigm of the planktonic food web. Kiel. Meeresforsch. (S)5, 1–28.

Zohary, T., Robarts, R.D., 1998. Experimental study of microbial P limitation in the eastern Mediterranean. Limnol. Oceanogr. 43, 387–395.